Stability of Nonlinear Time-Delay Systems Describing Human–Robot Interaction

Florian Müller , Jens Jäkel , Jozef Suchý, and Ulrike Thomas

Abstract—In this paper, we present sufficient conditions for the stability analysis of a stationary point for a special type of nonlinear time-delay systems. These conditions are suitable for analyzing systems describing physical human–robot interaction (pHRI). For this stability analysis a new human model consisting of passive and active elements is introduced and validated. The stability conditions describe parameterization bounds for the human model and an impedance controller. The results of this paper are compared to stability conditions based on passivity, approximated time-delays and to numerical approaches. As a result of the comparison, it is shown that our conditions are more general than the passivity condition of Colgate and Schenkel. This includes the consideration of negative stiffness and nonlinear virtual environments. As an example, a pHRI including a nonlinear virtual environment with a polynomial structure is introduced and also successfully analyzed. These theoretical results could be used in the design of robust controllers and stability observers in pHRI.

Index Terms—Impedance control, Lyapunov–Krasovskii functional, nonlinear time-delay systems, physical human–robot interaction (pHRI).

I. INTRODUCTION

IN PHYSICAL human–robot interaction (pHRI), a robot and a human share a common workspace and the human guides the robot via direct physical contact. This technology is based on sensing the forces and torques of the human's arm and the implementation of an impedance controller. The pHRI is used in industrial tasks for teaching procedures and lifting heavy objects. The stability analysis for a pHRI system is a complex problem. The reason for this lies in the difficulty of modeling

human behavior appropriately. A common approach is to use a mass-spring-damper system for the human model. Many authors use modifications of this model for their stability analysis [2]–[5]. An important additional aspect of human behavior is the response time [2], [6], [7]. Several authors implement response time in the form of a time-delay in their human models. Through this, the model is more precise however, the stability analysis becomes more complicated.

This paper begins with presenting an overview on human models in the context of pHRI including the passive biomechanical behavior and also the active human reactions. In Section II, the corresponding stability analysis is discussed. As the major result, we analytically derive stability conditions of a general polynomial nonlinear time-delay system applicable to pHRI, describing bounds for parameterization (see Section III). A new type of human model is introduced and validated in Section IV. In Section V, the stability conditions from Section III will be applied to a system describing pHRI with a human model with both passive and active parts. Here, a linear and a nonlinear case will be discussed and compared to other approaches. Section VI concludes the paper and gives an outlook on the practical use of the theoretical findings of this paper.

II. RELATED WORKS

Human models in the form of a mass-spring-damper system are widely used in haptic and pHRI research [8]–[10] due to the biomechanical properties of the human arm. The parameterization of the components have a wide range (see, e.g., [11] for an overview). The reason for this is the specific postures of the human arm when performing different tasks [5] and the intuitive strategies of humans to adapt their biomechanical impedance [12]. For this reason, some authors use robust human models [3]. However, assuming the mass of the human arm is significantly smaller in relation to the system mass, it is appropriate to neglect the mass of the human arm [13], [14] or additionally the damping of the arm (for a significantly smaller human damping) [2], [15], [16]. Other human models describe the human behavior as a PD-controller [4]–[6], which could be interpreted as an active spring-damper feedback.

In haptic research, the majority of authors assume that the interaction between the operator and the robot cannot lead to unstable behavior [17]. Their main focus lies on computational delays and delays in teleoperation systems [5]. This assumption is correct under the condition that the human reacts like a passive system [18]. However, it is shown in [19] that the operator could

be an active system that injects energy into the robotic system. This active feedback is described by negative parameters for the human impedance. This result was found in experiments with devices, which imposed perturbations to the pHRI. This effect occurs especially where rigid grasping of the handle is demonstrated. A comparable situation appears using a combination of impedance control and a virtual environment. These virtual environments are used in different applications such as rehabilitation [20]–[22] and industrial tasks [15], [16], [23] in the form of virtual springs, virtual walls or potential force fields. It is conceivable that a virtual environment provokes an active reaction of the human operator. Therefore, Müller *et al.* [15], [16] chose an active behavior in the form of a positive feedback of their human model.

Apart from the biomechanical impedance, the response time is an essential aspect of human behavior, especially in the case of an active human–robot interaction. The resulting time-delay is crucial for the stability as the example of a human body as an inverted pendulum shows [6]. Also in [5], by using a human model with time-delay, it is demonstrated that an operator can only stabilize the system under certain conditions. In [2], the authors use an approximation in the form of a low-pass filter to model the human response time.

The simulation study of [2] is used to analyze the influences of the model parameters on the stability of human–robot interaction. Müller *et al.* [15], [16] analyzed their system with the linear matrix inequality (LMI) approach of [24] and [25, p. 191] resulting in a numerical stability bound. Duchaine and Gosselin [13] derived analytical stability bounds in the case of a neglected response time. However, understanding the low-pass filter in front of their impedance controller as an approximated time-delay, the results can be compared to the results of this paper. In the same manner, it is also possible to consider the analytical solution of [9], which results in a more general case of [13] due to the stiffness in the impedance controller. Furthermore, it is possible to assume the time-delay as an all-pass filter by using the Padé-approximation [26]. The result is a higher order linear system. Its stability can be analyzed by using the Hurwitz criterion [27]. Higher orders of the Padé-approximation leads to more accurate approximations. With higher system orders, numerical solutions should be preferred, since the computing time increases exponentially to the system order. The passivity approach of [1] also gives an analytical solution that is suitable for analyzing active pHRI. The virtual environment in [1] could be treated as a human PD-controller behavior and the zero-order hold (ZOH) as an approximated time-delay.

Through the integration of a potential force field, the system describing pHRI could become nonlinear. A tunnel-shaped potential force field is presented in [15] and [16], in which the force is polynomial increasing depending on the distance from the zero point. This force field is used to guide an operator to a target while performing an industrial task. Furthermore, in [21], a similar type of nonlinear force field was applied to guide patients in a preferred movement by means of a hand exoskeleton for rehabilitation. Müller *et al.* [15], [16] proved the stability by using a Lyapunov function only in the case

of a neglected time-delay. Numerical solutions for the stability problem of nonlinear systems with time-delays could be found by using the sum of square method [28].

In summary, humans act in the context of pHRI as passive mass-spring-damper systems and they also react actively to forces and velocities in the form of a delayed PD-controller. The passive part as well as the active part of the behavior have an impact on the stability. Due to this, we present as the minor innovation of the paper, a delayed passive/active human model for pHRI. This model is a combination of different approaches to reenact the human behavior in a pHRI. The major contribution of this paper is the analysis of this human model with conditions found by an analytically stability proof for nonlinear time-delay systems.

III. STABILITY OF NONLINEAR TIME-DELAY SYSTEMS

We consider a stationary point of a special type of nonlinear time-delay systems. The proof for the resulting sufficient stability conditions for these systems is based on the Lyapunov–Krasovskii functional. The relation to pHRI is discussed in the following section.

Consider the following type of nonlinear time-delay systems

$$\dot{x} = Az + Bz(t - t_\mathrm{d}) \tag{1}$$

with the system matrices

$$A = \begin{pmatrix} a_{11} & a_{12} \\ 1 & 0 \end{pmatrix}, \quad B = \begin{pmatrix} b_{11} & b_{12} \\ 0 & 0 \end{pmatrix} \tag{2}$$

and the linear state vector and nonlinear vector

$$x = \begin{pmatrix} x_1 \\ x_2 \end{pmatrix} \quad \text{and} \quad z = \begin{pmatrix} x_1 \\ x_2|x_2|^{n-1} \end{pmatrix} \tag{3}$$

with $n \in \mathbb{R}^{\geq 1}$ and the delay t_d.[1]

Proposition I: The equilibrium $x_0 = [0 \;\; 0]^T$ of the system (1) is locally asymptotically stable, if the conditions

$$t_\mathrm{d} < -\frac{a_{11} + |b_{11}|}{|b_{12}|r^{n-1}n} \tag{4}$$

$$0 > a_{12} + b_{12} \text{ and} \tag{5}$$

$$r \geq |x_2| \tag{6}$$

with the parameter $r \in \mathbb{R}^+$, which defines the size of the region of attraction in state space are satisfied.

Proof: This proof is based upon the work of [29] and [25] where the Lyapunov–Krasovskii functional is used. For the stability proof, we use the so-called implicit model transformation. Consider the quadratic Lyapunov–Krasovskii functional candidate

$$V(x) = z^T(t)CPx(t) + \int_{t-t_\mathrm{d}}^{t} \int_{t+\theta}^{t} \dot{z}^T(\xi)F\dot{z}(\xi) \, \mathrm{d}\xi \, \mathrm{d}\theta$$

$$+ \int_{t-t_\mathrm{d}}^{t} z^T(t+\theta)Sz(t+\theta) \, \mathrm{d}\theta \tag{7}$$

[1]If n is odd, $z = (x_1 \;\; x_2{}^n)^T$.

with the positive definite two-dimensional (2-D) symmetric matrices S, F

$$C = \begin{pmatrix} 1 & 0 \\ 0 & \frac{2}{n+1} \end{pmatrix} \quad \text{and} \quad P = \begin{pmatrix} p_{11} & 0 \\ 0 & p_{22} \end{pmatrix}. \tag{8}$$

By considering that

$$\frac{\mathrm{d}}{\mathrm{d}t} z^T(t) C P x(t) = z_{0t_d}^T \begin{pmatrix} PA + A^T P & PB \\ B^T P & 0 \end{pmatrix} z_{0t_d} \tag{9}$$

$$\frac{\mathrm{d}}{\mathrm{d}t} \int_{t+\theta}^{t} \dot{z}^T(\xi) F \dot{z}(\xi) \, \mathrm{d}\xi = \dot{z}^T(t) F \dot{z}(t)$$
$$- \dot{z}^T(t+\theta) F \dot{z}(t+\theta) \tag{10}$$

$$\frac{\mathrm{d}}{\mathrm{d}t} \int_{t-t_d}^{t} z^T(t+\theta) S z(t+\theta) \, \mathrm{d}\theta = z_{0t_d}^T \begin{pmatrix} S & 0 \\ 0 & -S \end{pmatrix} z_{0t_d} \tag{11}$$

the derivative can be calculated as

$$\dot{V}(x) = z_{0t_d}^T \begin{pmatrix} PA + A^T P + S & PB \\ B^T P & -S \end{pmatrix} z_{0t_d}$$
$$+ t_d \dot{z}^T(t) F \dot{z}(t) - \int_{t-t_d}^{t} \dot{z}^T(t+\theta) F \dot{z}(t+\theta) \, \mathrm{d}\theta \tag{12}$$

where

$$z_{0t_d} = \left(z^T(t) \; z^T(t-t_d) \right)^T. \tag{13}$$

For eliminating the last term of the right-hand side of (12), we introduce

$$0 \leq \int_{t-t_d}^{t} z_{0\dot{\theta}}^T \begin{pmatrix} D & E \\ E^T & F \end{pmatrix} z_{0\dot{\theta}} \, \mathrm{d}\theta$$
$$= t_d z^T(t) D z(t) + 2 z^T(t) E(z(t) - z(t-t_d))$$
$$+ \int_{t-t_d}^{t} \dot{z}^T(t+\theta) F \dot{z}(t+\theta) \, \mathrm{d}\theta. \tag{14}$$

With

$$z_{0\dot{\theta}} = \left(z^T(t) \; \dot{z}^T(t+\theta) \right)^T \tag{15}$$

and the 2-D matrices $D^T = D$ and E satisfying

$$\begin{pmatrix} D & E \\ E^T & F \end{pmatrix} > 0. \tag{16}$$

This formulation is given in [25, p. 174] and based on [29] with using the cost function of [30]. Adding (12) and (14), we eliminate the integral term of (12) and obtain

$$\dot{V}(x) \leq z_{0t_d}^T \begin{pmatrix} \Lambda & PB - E \\ B^T P - E^T & -S \end{pmatrix} z_{0t_d}$$
$$+ t_d \dot{z}^T(t) F \dot{z}(t) \tag{17}$$

with

$$\Lambda = PA + A^T P + t_d D + E + E^T + S \tag{18}$$

$$D = \begin{pmatrix} d_{11} & 0 \\ 0 & 0 \end{pmatrix}, \quad E = \begin{pmatrix} 0 & p_{11} b_{12} \\ 0 & 0 \end{pmatrix} \tag{19}$$

$$F = \begin{pmatrix} 0 & 0 \\ 0 & f_{22} \end{pmatrix}, \quad S = \begin{pmatrix} s_{11} & 0 \\ 0 & 0 \end{pmatrix} \tag{20}$$

and $p_{22} = -p_{11}(a_{12} + b_{12})$ \hfill (21)

to obtain

$$0 \geq z_{0t_d}^T \begin{pmatrix} 2a_{11}p_{11} + t_d d_{11} + s_{11} & 0 & p_{11}b_{11} & 0 \\ 0 & 0 & 0 & 0 \\ p_{11}b_{11} & 0 & -s_{11} & 0 \\ 0 & 0 & 0 & 0 \end{pmatrix} z_{0t_d}$$
$$+ t_d \dot{z}^T(t) F \dot{z}(t). \tag{22}$$

With the weak derivative[2] by using $\dot{x}_2(t) = x_1(t)$

$$\dot{z} = \left(\dot{x}_1(t) \; n|x_2(t)|^{n-1} x_1(t) \right)^T \tag{23}$$

we get

$$0 \geq (2a_{11}p_{11} + t_d d_{11} + s_{11}) \, x_1^2(t)$$
$$+ \left(t_d n^2 |x_2(t)|^{2n-2} \right) f_{22} x_1^2(t)$$
$$+ 2p_{11}b_{11}x_1(t)x_1(t-t_d) - s_{11}x_1^2(t-t_d). \tag{24}$$

With

$$f_{22} = \frac{1}{t_d n^2 r^{2n-2}}, r \in \mathbb{R}^+ \tag{25}$$

it follows

$$0 \geq (2a_{11}p_{11} + t_d d_{11} + s_{11}) \, x_1^2(t) + \left(\frac{|x_2|}{r} \right)^{2n-2} x_1^2(t)$$
$$+ 2p_{11}b_{11}x_1(t)x_1(t-t_d) - s_{11}x_1^2(t-t_d). \tag{26}$$

With the restrictions $|x_2(t)| \leq r$ and $n \geq 1$

$$\left(\frac{|x_2(t)|}{r} \right)^{2n-2} \in [0, 1]. \tag{27}$$

Now, we can state that the critical case of (27) is the upper bound 1 and this case will be used for the inequality

$$0 \geq z_{0t_d}^T \begin{pmatrix} \kappa & 0 & p_{11}b_{11} & 0 \\ 0 & 0 & 0 & 0 \\ p_{11}b_{11} & 0 & -s_{11} & 0 \\ 0 & 0 & 0 & 0 \end{pmatrix} z_{0t_d} \tag{28}$$

with

$$\kappa = 2a_{11}p_{11} + t_d d_{11} + s_{11} + 1 \tag{29}$$

which is satisfied for $|x_2| \leq r$. The 1 of the critical case appears in the first term of (28).

From the analysis of the eigenvalues of the matrix of (28), we get

$$-(2a_{11}p_{11} + t_d d_{11} + s_{11} + 1)s_{11} \leq (p_{11}b_{11})^2. \tag{30}$$

---

[2]If n is odd, it is possible to use the ordinary derivative.

To find the s_{11}, which gives the largest value of the left-hand side of (30), we have to solve the associated maximization problem resulting in

$$s_{11} = -a_{11}p_{11} - \frac{1}{2}t_d d_{11} - \frac{1}{2} \text{ and} \tag{31}$$

$$a_{11}p_{11} + \frac{1}{2}t_d d_{11} + \frac{1}{2} \leq \mp p_{11}|b_{11}|. \tag{32}$$

Summarizing, the system (1) is stable if $P > 0$, $|x_2| \leq r$ and condition (16) and (32) are satisfied.

To obtain the stability conditions of Proposition I, we have to introduce some simplifications. At first, from the analysis of the eigenvalues of (16), we get $d_{11}f_{22} > (p_{11}b_{12})^2$. With (25), it follows

$$d_{11} > t_d(p_{11}b_{12}nr^{n-1})^2 \tag{33}$$

and from condition (32), we obtain

$$d_{11} \leq \frac{-2(a_{11} \pm |b_{11}|)p_{11} - 1}{t_d}. \tag{34}$$

We see that if $p_{11} > 0$ and d_{11} is inside the bounds of (33) and (34) the system is stable. From this, we derive the stability bounds

$$\frac{-2(a_{11} \pm |b_{11}|)}{p_{11}} - \frac{1}{p_{11}^2} > (t_d b_{12}nr^{n-1})^2. \tag{35}$$

Finding the maximum of the left-hand side of (35) with respect to p_{11} results in

$$p_{11} = -\frac{1}{a_{11} \pm |b_{11}|}. \tag{36}$$

From inserting (36) in (35), we obtain

$$\pm(a_{11} \pm |b_{11}|) > t_d|b_{12}|nr^{n-1}. \tag{37}$$

The Lyapunov condition requires $P > 0$, which results in

$$a_{11} \pm |b_{11}| < 0 \text{ and} \tag{38}$$

$$a_{12} + b_{12} < 0. \tag{39}$$

Condition (38) eliminates the positive solution on the left-hand side of (37) and we obtain

$$-(a_{11} \pm |b_{11}|) > t_d|b_{12}|nr^{n-1}. \tag{40}$$

This includes two conditions and both have to be fulfilled for stability. As the condition with the $+|b_{11}|$ term is more conservative than the one with $-|b_{11}|$ only the first has to be considered in the following. Further, by proofing $S > 0$ it can be shown that (31) becomes a special case of (34), which results for $b_{11} = 0$. Finally, we obtain the three conditions

$$-(a_{11} + |b_{11}|) > t_d|b_{12}|nr^{n-1} \tag{41}$$

$$a_{12} + b_{12} < 0 \text{ and} \tag{42}$$

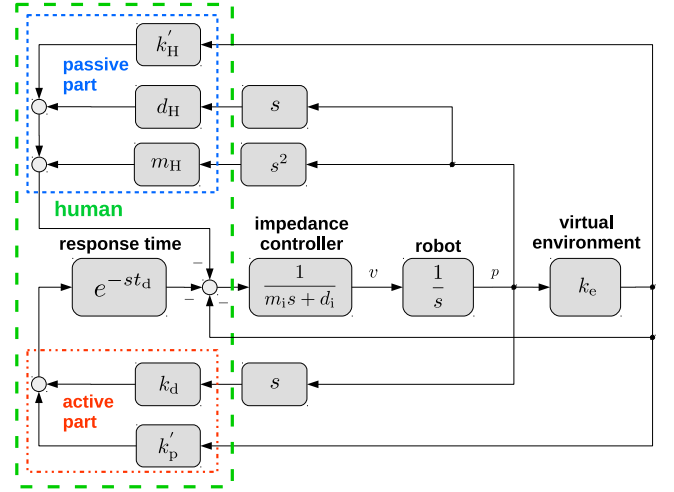$$|x_2| \leq r \tag{43}$$

for stability.

Fig. 1. Block diagram for physical human–robot interaction with a passive/active human model consisting of a passive mass-spring-damper system and delayed PD-controller behavior.

The derivative of the Lyapunov functional (7) has the form

$$\dot{V}(x) \leq \left(\frac{-a_{11}}{a_{11} + |b_{11}|} + \frac{1}{2} \left(\frac{b_{12}t_d nr^{n-1}}{a_{11} + |b_{11}|} \right)^2 \right.$$
$$\left. + \frac{1}{2} \left(\frac{|x_2(t)|}{r} \right)^{2n-2} \right) \cdot \left(x_1^2(t) + x_1^2(t - t_d) \right)$$
$$- \frac{2b_{11}}{a_{11} + |b_{11}|} x_1(t)x_1(t - t_d) \tag{44}$$

for all $|x_2| < r$.

To proof the asymptotic stability we use the invariant set theorem [31]. This implies that if

$$\dot{x}_1 = a_{11}z_1(t) + a_{12}z_2(t) + b_{11}z_1(t - t_d) + b_{12}z_2(t - t_d) \neq 0 \tag{45}$$

with $t \to \infty$, $z_1(t) = 0$, $z_1(t - t_d) = 0$, $z_2(t) \neq 0$, and $z_2(t - t_d) \neq 0$ the solution is asymptotically stable. This results in

$$z_2(t) \neq \frac{b_{12}}{-a_{12}} z_2(t - t_d). \tag{46}$$

This condition could only be temporally violated since $z_2(t - t_d)$ follows $z_2(t)$. Therefore, $z(t - t_d)$ will change if $z(t) \neq z(t - t_d)$ and if $z(t) = z(t - t_d)$ condition (46) would be $-a_{12} \neq b_{12}$, which is fulfilled by condition (5). From this, we can deduce that for $t \to \infty$ (46) is fulfilled and the system is asymptotically stable. ∎

IV. HUMAN MODEL

A. Model Description

We consider a 1-D pHRI system including an impedance controller with a virtual mass m_i and a virtual damping d_i (see Fig. 1). For simplification the actuator dynamics of the robot will be neglected and, thus, the robot is represented by an integrator. Furthermore, we consider a virtual environment in the form of a

stiffness k_e. As a conclusion of Section II, for the human model a passive and an active part are considered.

The passive part consists of the mass m_H, the damping d_H and the stiffness of the human arm k_H. The passive stiffness k_H is in our assumption an offset tension of the arm muscles. It is correlated to the expected movement of the mechanical device. Another way, how passive stiffness could occur is reaching joint limits of the human arm. However, this will not be considered in our model. This means the stiffness is defined by $k_H = k_H' k_e$ with the factor k_H' the human stiffness is proportional to the stiffness of the virtual environment k_e. This also implies that for $k_e = 0$ also $k_H = 0$, which means all stiffness disappears from the system.

The active part of the human model describes a reaction to the force of the virtual environment and to the system velocity. This could be interpreted as a PD-controller with the proportional gain $k_p = k_p' k_e$ and the derivation gain k_d. In [6], the controller is also denoted as a virtual active spring and damper. The controller is delayed by the human response time t_d in form of a time-delay. For simplification, this parameter is assumed to be fixed since the variation has a slow dynamic.

A reaction to the position of the robot occurs only indirectly over the virtual environment. In [32], the authors assume that humans can create potential force fields in their minds. From that, we can deduce that if no virtual environment exists and humans want to follow a path, they create a force field, which guides them to the path. With this assumption path following can be described by our model. However, for stability analysis only a stationary point is considered.

In contrast to [18], we assume that the three passive parameters are fixed in a given work task. Furthermore, it is conceivable that due to training humans can adapt their active control parameters in certain limits to stabilize the system. For the following stability analysis all parameters are assumed as fixed during a task. This simplification is necessary for using the proposed stability conditions.

With this assumption, we derive the state space model

$$\dot{x} = \begin{pmatrix} -\frac{d}{m} & -\frac{k}{m} \\ 1 & 0 \end{pmatrix} x + \begin{pmatrix} -\frac{k_d}{m} & -\frac{k_p}{m} \\ 0 & 0 \end{pmatrix} x(t - t_d) \qquad (47)$$

with the state vector $x = [v\ p]^T$, the velocity v, the position p, and the response time t_d. Further, the overall mass, damping and stiffness are defined by

$$m = m_i + m_H \qquad (48)$$

$$d = d_i + d_H \qquad (49)$$

$$k = k_e + k_H. \qquad (50)$$

B. Model Validation

For the validation of the passive/active human model and a comparison of the passive and the active model, we identified the model parameters for participants of a user study in all three cases. The hypothesis is that the passive/active model fits measured data better than the other two models.

For this purpose, a 1-D pHRI experimental setup according to block diagram of Fig. 1 was designed. The participants of the
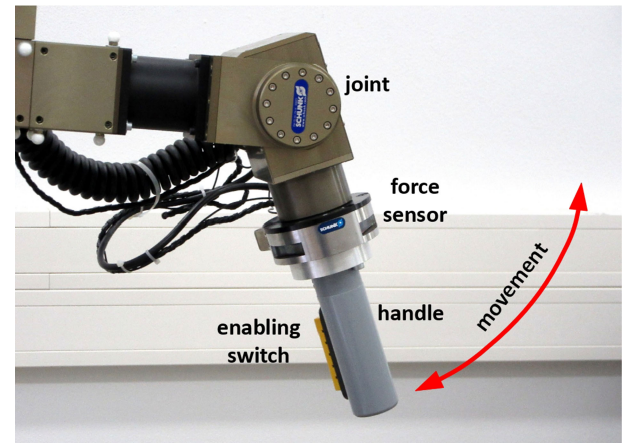

Fig. 2. Experimental setup: Joint in target position.

study had to position the robot TCP by moving a single joint of a kinematic chain using an impedance controller (see Fig. 2). The impedance controller is implemented in joint space and is parameterized with inertia $m_i = 2\,\mathrm{kgm}^2$ and damping $d_i = 3\,\mathrm{kgm}^2/s$. The value of the damping was chosen on the basis of the ratio of the user's expected maximum torques to the desired maximum angular velocity. For the mass, we chose a value that results in a comfortable dynamical behavior. In addition, the impedance controller is combined with a linear potential force field with $k_e = 0.25\,\mathrm{Nm}/°$, which has an equilibrium at $q_0 = 20°$.

For the study five students and employees of the Leipzig University of Applied Science (5 male, 0 female, age: mean = 28.8 years, standard deviation = 5.0 years, range: [24 – 37] years) were recruited.

This study is designed as follows. The participant grasps the handle (see Fig. 2). The joint is in the start position with $q_S = 60°$. By pushing the enabling switch at the handle the participant starts a trial. The potential force field guides the user to the equilibrium. The participants are instructed to find the equilibrium as fast as possible. The duration for one trial is 10 s. This study is organized as a competition. We assume that this design describes more realistically the human behavior in a pHRI as a design without a work instruction. Every participant carried out 20 trials.

The model parameters are identified for all three models minimizing the mean squared deviation between the measured and the simulated joint angle. In the optimization, the parameters are restricted with all passive parameters being positive and the response time being between 0.2 s and 0.4 s. Furthermore, the mass of the human arm is restricted by $m_H \leq 7\,\mathrm{kg}$.

Table I contains the mean and the standard deviation of the human parameters and the best fit of the mean squared error for all participants depending on the used human model. The standard deviation of the human parameters of all participants is rather large. The reason for this is first the individual reaction in every trial and the learning effect of every participant. Second, the parameters were not measured, they just represent the best fit. Parameterizations with similar fits could be much different.

TABLE I
RESULTS FOR THE EXPERIMENTAL VALIDATION OF THE HUMAN MODELS

PN	model	$\frac{m_H}{kg}$	$\frac{d_H}{kg/s}$	k'_H	$\frac{k_d}{kg/s}$	k'_p	$\frac{t_d}{s}$	best fit
1	P/A M	3.9	5.5	1.6	2.2	-0.3	0.34	0.27
	(SD)	(2.0)	(10.4)	(0.8)	(4.7)	(1.5)	(0.08)	(0.08)
	A M	-	-	-	1.4	-0.0	0.22	0.35
	(SD)	-	-	-	(0.7)	(0.1)	(0.04)	(0.12)
	P M	2.8	8.5	1.8	-	-	-	0.36
	(SD)	(8.4)	(1.0)	(2.4)	-	-	-	(0.13)
2	P/A M	4.0	4.9	1.7	3.6	-0.3	0.32	0.42
	(SD)	(2.9)	(7.7)	(1.0)	(6.2)	(1.6)	(0.08)	(0.31)
	A M	-	-	-	1.9	0.0	0.28	0.48
	(SD)	-	-	-	(1.0)	(0.1)	(0.07)	(0.32)
	P M	2.1	8.3	1.7	-	-	-	0.64
	(SD)	(1.9)	(1.0)	(15.0)	-	-	-	(0.41)
3	P/A M	4.1	2.7	1.7	2.3	-0.9	0.35	0.47
	(SD)	(2.1)	(6.9)	(0.9)	(3.6)	(1.3)	(0.07)	(0.34)
	A M	-	-	-	0.4	-0.3	0.30	0.60
	(SD)	-	-	-	(1.7)	(0.3)	(0.09)	(0.40)
	P M	2.5	9.8	1.6	-	-	-	0.94
	(SD)	(1.8)	(6.3)	(1.1)	-	-	-	(1.09)
4	P/A M	3.4	8.6	1.4	0.8	-0.5	0.32	0.11
	(SD)	(2.3)	(12.3)	(1.0)	(4.7)	(2.1)	(0.08)	(0.09)
	A M	-	-	-	1.7	-0.3	0.23	0.23
	(SD)	-	-	-	(1.6)	(0.2)	(0.07)	(0.13)
	P M	1.2	10.9	1.1	-	-	-	0.31
	(SD)	(0.7)	(3.3)	(0.4)	-	-	-	(0.22)
5	P/A M	3.9	2.0	1.5	3.5	-0.9	0.37	1.07
	(SD)	(5.1)	(6.2)	(2.0)	(6.5)	(2.6)	(0.08)	(0.41)
	A M	-	-	-	0.6	-0.3	0.36	1.26
	(SD)	-	-	-	(1.9)	(0.4)	(0.04)	(0.44)
	P M	3.1	12.5	2.4	-	-	-	1.88
	(SD)	(2.6)	(6.2)	(1.5)	-	-	-	(0.91)

Legend: PN – participants number, M – mean, *SD* – standard deviation, P/A – passive/active model, P – passive model, A – active model
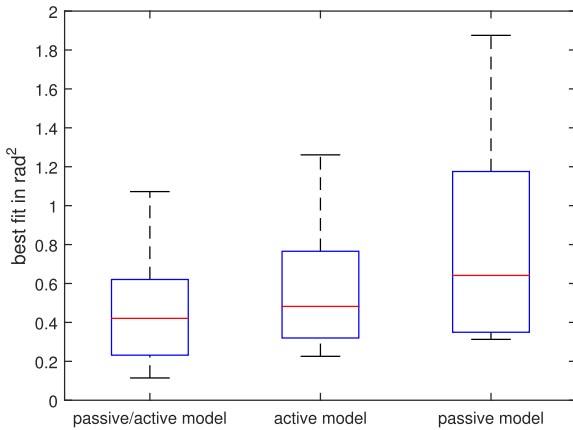

Fig. 3. Box-and-whiskers plot of the best fit of the three human models.

Fig. 3 shows a box-and-whiskers plot of the best fit from the results of the three human models. Both models with an active part significantly better fit the measured data than the passive model. This indicates that in the contexts of pHRI models describing delayed active human reactions are more appropriate than pure passive models. Furthermore, the passive/active model shows the best fit of all three models as hypothesized. Fig. 4 gives exemplary the experimental result of one trial with the corresponding simulation results for the best fitting parameterization for the three types of human models. The two models with an active part clearly outperform the passive human model.
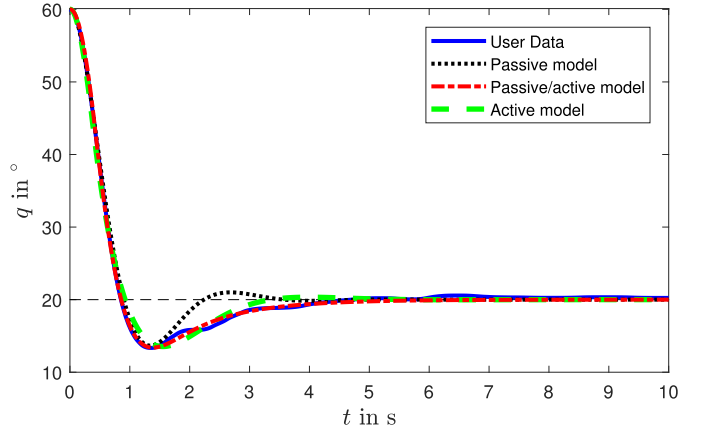

Fig. 4. Example for comparison of the different human models: Trial 1 of participant 4, passive model parameters: $m_H = 1.9\,\text{kg}$, $d_H = 8.0\,\text{kg/s}$, $k'_H = 1.0$, active model parameters: $k_d = -1.3\,\text{kg/s}$, $k'_p = -0.6$, $t_d = 0.36\,\text{s}$, passive/active model parameters: $m_H = 7.0\,\text{kg}$, $d_H = 0.0\,\text{kg/s}$, $k'_H = 2.5$, $k_d = 0.08\,\text{kg/s}$, $k'_p = -2.6$, $t_d = 0.38\,\text{s}$.

V. DISCUSSION

A. Linear Case

For the system (47), Proposition I with $n = 1$ in (3) can be applied. Since (47) is linear for $n = 1$, only the first two conditions of the proposition have to be checked. This results in the two conditions of the first line of Table II. All three passive human parameter increase the stability region. The stability conditions are independent of the mass. The increase of the response time and the control parameters result in a smaller stability region. It is clear that both active human parameters k_d and k_p could also be negative due to the absolute value function. In this case the human inserts energy into the system and the system is still asymptotically stable. The condition demonstrates that the presence of active human reactions with a response time affects the stability of pHRI. With Condition 1, the stability of an impedance controller can be guaranteed by choosing a corresponding damping d_i. Condition 2 demands that the sum of all stiffness in the system has to be positive. The condition is fulfilled when the user is able to find the equilibrium. If the user drifts away, the condition is violated. This condition is a theoretical result and has no relevant information for the parameterization of a controller.

The table also contains the Passivity condition of Colgate [1], which we adapt to the context of pHRI. For this, the time-delay is approximated by half of the sample time $t_d = T/2$. We also adapted the stability condition of Hulin *et al.* [9] and Duchaine and Gosselin [13] by interpreting the time constant of the low-pass filter as time-delay. In addition, the table contains a stability condition determined by the Hurwitz criterion [27] for a system with a first-order Padé-approximated time-delay. The passivity condition and the Proposition I show a high similarity. However, the passivity condition is much more conservative than that of Proposition I. The conditions of [9] and [13] and the result of the Hurwitz criterion are much more complex than the other two stability conditions. In contrast to Proposition I and the passivity

TABLE II
LINEAR STABILITY CONDITIONS FOR pHRI WITH A HUMAN MODEL WITH PASSIVE AND ACTIVE ELEMENTS

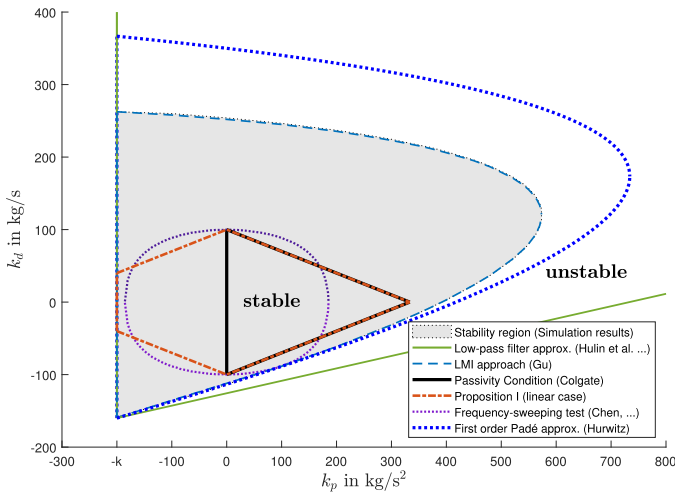|	Time-delay	Condition 1	Condition 2
Proposition I with $n = 1$	exact time-delay	$d - |k_d| > t_d |k_p|$	$k + k_p > 0$
Passivity condition (Colgate [1])	approx. of zero-order hold	$d - |k_d| > t_d k_p$	–
Hulin *et al.* [9] and Duchaine and Gosselin [13]	approx. as low-pass filter	$\left(\dfrac{t_d d}{m} + 1 \right)(d + k_d) > t_d k_p - \dfrac{k t_d^2 d}{m}$	$k + k_p > 0$
Hurwitz criterion [27]	approx. as all-pass filter	$(2m + t_d(d - k_d))(2(d + k_d) + t_d(k - k_p)) > 2m t_d(k + k_p)$	$k + k_p > 0$

Fig. 5. Stability bounds for parameterization $m = 40$ kg, $d = 100$ kg/s, $k = 200$ kg/s^2, and $t_d = 0.3$ s.

TABLE III
NUMERICAL EXAMPLES FOR STABLE PARAMETERS FOR THE PASSIVE HUMAN PARAMETERS $d_H = 5$ kg/s AND $k'_H = 1.5$ USING THE LINEAR PROP. I OF TABLE II

$k_d = 1$ kg/s, $k'_p = -0.1$, $t_d = 0.2$ s		$k_d = 3$ kg/s, $k'_p = -0.5$, $t_d = 0.4$ s	
k_e	d_i	k_e	d_i
10 N/m	> -3.8 kg/s	10 N/m	> 0 kg/s
20 N/m	> -3.6 kg/s	20 N/m	> 2 kg/s
40 N/m	> -3.2 kg/s	40 N/m	> 6 kg/s
100 N/m	> -2.0 kg/s	100 N/m	> 18 kg/s
400 N/m	> 4.0 kg/s	400 N/m	> 78 kg/s

condition, studies [9], [13] and the result of the Hurwitz criterion are dependent on the mass. The mass has a significant influence on the stability margin. Another difference to Proposition I and the passivity condition is the higher stability margin due to the active human damping k_d. The similarities of all conditions are the increase of robustness by an increasing overall damping d and a decrease by an increasing absolute value of the active human stiffness k_p.

For a graphical comparison (see Fig. 5). In addition to the conditions listed in Table II, the figure also shows the stability bound of the numerical LMI approach [24] for time-delay systems with Proposition 5.22 from [25], the stability regions determined by simulations of a continuous system with a time-delay and the Frequency-sweeping test (FST) [33]. The figure shows the stability bounds in k_p-k_d plane. The impedance controller is parameterized with $m_i = 39$ kg and $d_i = 90$ kg/s. The virtual environment is defined by $k_e = 160$ kg/s^2. For the passive human parameters the following assumptions are made: $m_H = 1$ kg, $d_H = 10$ kg/s, $k_H = 40$ kg/s^2. Furthermore, for the human response time $t_d = 0.3$ s is assumed. The numerical LMI approach corresponds quite well to the stability region. The linear case of Proposition I is completely included in the stability region. However, the condition is clearly more conservative than

the numerical approaches. The reason for this is that in the proof of Proposition I P in (8) is just a diagonal matrix and also the matrices (19) and (20) have a special structure with few freely selectable parameters. The FST is also involved in the stability region. However, the stability bound of FST are different from the ones used in Proposition I. Furthermore, condition $k + k_p > 0$ corresponds to the exact stability bound (see at $k_p = -k$ in Fig. 5). The conditions under which the time-delay is approximated by a low-pass filter and by an all-pass filter violate the stability region obtained by simulation. This shows clearly the unsuitability of low-pass and all-pass filter approximations of a response time for stability analysis in the context of pHRI.

Table III shows some numerical examples of different parameter settings for Condition 1 in the first row of Table II. The left part of the table contains an optimistic setting for the active human parameters, the right part, a more conservative setting. Both settings are based on the experimental results of Table I. By varying the virtual stiffness k_e, we obtain different limits for the damping of the impedance controller d_i. The table shows clear differences in parameter settings for different assumptions on the human parameters. The negative parameterization of the damping of the impedance controller is possible because of the passive damping of the human arm d_H. Such negative damping could occur when using a variable impedance controller (see [34]). The table demonstrates the benefit and also the difficulty of using Proposition I for pHRI.

To consider Proposition I for systems, which includes a ZOH element like in [9] and [1], we have to introduce the sampling time T. The hold part will be approximated by half of the sampling time $T/2$ [9], which will be added to the time-delay
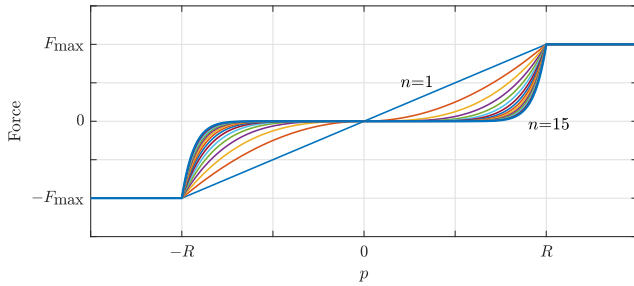
Fig. 6. Progression of the nonlinear force field for $n = 1 \ldots 15$ by [15], [16].

of Proposition I. We obtain

$$d - |k_d| > \left(t_d + \frac{T}{2} \right) |k_p| \quad \text{and} \quad k + k_p > 0. \tag{51}$$

For $t_d = 0$ and $k = 0$ (51) corresponds to the original passivity condition of [1]

$$d - |k_d| > \frac{k_p T}{2}. \tag{52}$$

Finally, it can be shown that condition (51) is in every stability limit given in the simulation study of [17].

B. Nonlinear Case

A suitable application that could be analyzed by Proposition I is the nonlinear system in [15] and [16]. The system describes a pHRI with an active human model in which the human operator is assisted by a tunnel-shaped potential force field with a polynomial behavior. This type of force field is used for guiding users of hand-guided robots to a given reference path to increase their performance and the user comfort of the system. Fig. 6 illustrates the progression of the potential force field. The force field has a radius R whereat the force is restricted by a maximum force F_{max}. The progression is described by an exponent n. With $n = 1$ within the region $|p| \leq R$ the linear case results. Using a higher value for n improves the settling time of the system. However, it also results in a larger control deviation [15], [16]. Such a force field could also be used for collision avoidance with joint limits or obstacles.

The human model has an active behavior in the form of a P-controller with the time-delay. This means the human reacts to the potential force field via feedback with the gain factor k'_p. The passive elements of the human model are not considered because it is assumed that they are significantly smaller than the impedance parameters and the force field stiffness. Also the derivative term of the human controller is not considered. In [16], this approximation of human behavior was validated in a user study.

For the stability analysis, the restriction of the maximum force will be neglected. Due to the rotational symmetry of the tunnel-shaped potential force field only one dimension in Cartesian space will be considered.

TABLE IV
PARAMETERIZATION RULES FOR FORCE FIELDS OF [15], [16]

	$d_i = 500 \, \mathrm{kg/s}, \ k'_p = -0.1$	$d_i = 130 \, \mathrm{kg/s}, \ k'_p = -0.5$
R	$4 \, \mathrm{cm} - 8 \, \mathrm{cm}$	$7.5 \, \mathrm{cm} - 11 \, \mathrm{cm}$
n	$2 - 4$	$2 - 4$
F_{max}	$20 \, \mathrm{N} - 35 \, \mathrm{N}$	$20 \, \mathrm{N} - 30 \, \mathrm{N}$

The system will be described by (1) with system matrices

$$A = \begin{pmatrix} -\dfrac{d_i}{m_i} & -\dfrac{F_{max}}{m_i R^n} \\ 1 & 0 \end{pmatrix} \quad \text{and} \quad B = \begin{pmatrix} 0 & -k'_p \dfrac{F_{max}}{m_i R^n} \\ 0 & 0 \end{pmatrix} \tag{53}$$

and the vectors

$$x = \begin{pmatrix} v \\ p \end{pmatrix} \quad \text{and} \quad z = \begin{pmatrix} v \\ p|p|^{n-1} \end{pmatrix} \tag{54}$$

with $n \in \mathbb{R}$, $n \geq 1$, velocity v and position p. This model corresponds to the model of the linear case (see Fig. 1). In the nonlinear case, instead of $k_e p$ for the virtual environment $k_e p |p|^{n-1} = F_{max}/R^n p |p|^{n-1}$ is used to describe the potential force field of Fig. 6.

Using Proposition I, the system is locally asymptotically stable if $|p| \leq R$

$$\frac{d_i}{t_d |k'_p|} > \frac{F_{max} n}{R} \quad \text{and} \quad k'_p > -1. \tag{55}$$

For r, we use the radius R because for $|p| > R$ the actual system is restricted. In this way, the stationary point of the system is globally asymptotically stable.

In the resulting condition (55) every parameter has the same weight. The increase of damping and radius increases the stability region and the increase of the maximum force, the response time, the absolute value of the active human stiffness and the exponent n decreases the stability region. This corresponds in large parts with the results of the simulation and experimental studies in [15] and [16]. The main difference is that the stability conditions of this paper show a higher stability margin for small n. In contrast, the simulation and experimental results show slower oscillations for an increasing n, indicating a larger stability margin. This leads to the assumption that for increasing n Proposition I becomes more conservative due to the conservative estimate of (27). The condition $k'_p > -1$ corresponds to a situation where the human operator accepts the guidance by the force field. Otherwise, the equilibrium will not be reached.

The results of the simulation and experimental studies in [15] and [16] lead to rules for a suitable parameterization of the force field. For different impedance parameters and different assumptions of the human gain factor nearly the same parameterization rules resulted (see Table IV). The critical parameters in this table are the small values of R, n and the high values of F_{max}. By verifying the rules with (55) and example parameters d_i, k'_p, n, and R of Table V, we obtain the stability bounds for parameter F_{max} (see Table V). The gray cells of the table show parameter values, which do not meet the full range of the parameterization

TABLE V
EXAMPLES FOR STABLE PARAMETERS FOR A HUMAN RESPONSE TIME OF $t_d = 0.3$ S USING PROPOSITION I

$d_i = 500\,\mathrm{kg/s},\ k_p' = -0.1$			$d_i = 130\,\mathrm{kg/s},\ k_p' = -0.5$		
R	n	$F_{\max}$	R	n	$F_{\max}$
4 cm	2	<333 N	7.5 cm	2	<32 N
4 cm	4	<166 N	7.5 cm	4	<16 N
6 cm	3	<333 N	9 cm	3	<26 N
8 cm	2	<666 N	11 cm	2	<47 N
8 cm	4	<333 N	11 cm	4	<23 N

rules of Table IV. Finally, we can summarize that the stability conditions confirm the parameterization rules for $n = 2$, but for $n > 2$ the parameter bounds resulting from (55) are rather conservative.

The results demonstrate that Proposition I is suitable for pHRI with active and passive/active human models, which also could include a potential force fields with a nonlinear polynomial description.

VI. CONCLUSION

In this paper, we derived stability conditions for a special type of nonlinear time-delay systems by using the Lyapunov–Krasovskii functional. We have shown that these conditions could be applied for analyzing physical human–robot interaction. The human operator is modeled as a combination of a passive mass-spring-damper system and an active PD-controller behavior with a time-delay. This human model was validated in a user study. It turned out that the introduced passive/active model describes human behavior better than an only passive or only active human model. The results show also a wide range of human parameters.

For the linear case the stability conditions are compared to other analytical and numeric approaches. We found that our conditions are a more general case of Colgates passivity condition. Furthermore, it has been shown that approaches using response time approximated by a low-pass filter or an all-pass filter detect false positive stability region. Finally, by introducing a tunnel-shaped nonlinear force field, a nonlinear system results and is successfully analyzed. It is shown that our stability conditions are more conservative than numerical approaches, especially for the nonlinear case.

In future work more applications based on the presented solution will be researched. Teleoperating systems are promising candidates. Also, the practical usability has to be investigated. For example, the solution could be used for parameterization of impedance controllers and also be a part of a stability observer for pHRI applications. A stability observer like this, based on the ideas of this paper, is described in [35]. The active human parameters are estimated online. The problem with the wide range of other human parameters is solved by using conservative assumptions for the parameterization. Furthermore, an extension of Proposition I for more complex robotic systems should be researched.

REFERENCES

[1] J. E. Colgate and G. Schenkel, "Passivity of a class of sampled-data systems: Application to haptic interfaces," *J. Robot. Syst.*, vol. 14, no. 1, pp. 38–47, Jan. 1997.

[2] T. Tsumugiwa, R. Yokogawa, and K. Yoshida, "Stability analysis for impedance control of robot for human-robot cooperative task system," in *Proc. IEEE/RSJ Int. Conf. Intell. Robots Syst.*, Sep. 2004, vol. 4, pp. 3883–3888.

[3] S. P. Buerger and N. Hogan, "Complementary stability and loop shaping for improved human-robot interaction," *IEEE Trans. Robot.*, vol. 23, no. 2, pp. 232–244, Apr. 2007.

[4] K. Kurihara, S. Suzuki, F. Harashima, and K. Furuta, "Human adaptive mechatronics (HAM) for haptic system," in *Proc. 30th IEEE Annu. Conf. Ind. Electron. Soc.*, Nov. 2004, vol. 1, pp. 647–652.

[5] L. L. Kovács and J. Kövecses, "Dynamics of coupled haptic systems," in *Proc. IEEE World Haptics Conf.*, Jun. 2015, pp. 286–292.

[6] G. Stepan, "Delay effects in the human sensory system during balancing," *Philosoph. Trans. Roy. Soc.*, vol. 367, no. 1891, pp. 1195–1212, Mar. 2009.

[7] T. C. Franklin, K. P. Granata, M. L. Madigan, and S. L. Hendricks, "Linear time-delay methods and stability analyses of the human spine. Effects of neuromuscular reflex response," *IEEE Trans. Neural Syst. Rehabil. Eng.*, vol. 16, no. 4, pp. 353–359, Aug. 2008.

[8] M. S. Erden and A. Billard, "End-point impedance measurements at human hand during interactive manual welding with robot," in *Proc. IEEE Int. Conf. Robot. Autom.*, May 2014, pp. 126–133.

[9] T. Hulin, C. Preusche, and G. Hirzinger, "Stability boundary for haptic rendering: Influence of human operator," in *Proc. IEEE/RSJ Int. Conf. Intell. Robots Syst.*, Sep. 2008, pp. 3483–3488.

[10] F. Dimeas and N. Aspragathos, "Online stability in human-robot cooperation with admittance control," *IEEE Trans. Haptics*, vol. 9, no. 2, pp. 267–278, Apr.–Jun. 2016.

[11] J. J. Gil, A. Avello, Á. Rubio, and J. Flórez, "Stability analysis of a 1 dof haptic interface using the Routh–Hurwitz criterion," *IEEE Trans. Control Syst. Technol.*, vol. 12, no. 4, pp. 583–588, Jul. 2004.

[12] F. Stulp, J. Buchli, A. Ellmer, M. Mistry, E. Theodorou, and S. Schaal, "Reinforcement learning of impedance control in stochastic force fields," in *Proc. IEEE Int. Conf. Develop. Learn.*, Aug. 2011, vol. 2, pp. 1–6.

[13] V. Duchaine and C. Gosselin, "Investigation of human-robot interaction stability using Lyapunov theory," in *Proc. IEEE Int. Conf. Robot. Autom.*, May 2008, pp. 2189–2194.

[14] K. Mohammadi, H. A. Talebi, and M. Zareinejad, "Lyapunov stability analysis of a bilateral teleoperation system interacting with active environment," in *Proc. 3rd RSI Int. Conf. Robot. Mechatronics*, Oct. 2015, pp. 96–101.

[15] F. Müller, J. Jäkel, and J. Suchý, "Tunnel-shaped potential force fields for improved hand-guiding of robotic arms," in *Proc. 20th Int. Conf. Methods Models Autom. Robot.*, Aug. 2015, pp. 429–434.

[16] F. Müller, J. Jäkel, U. Thomas, and J. Suchý, "Intuitive Handführung von Robotern als Handlingsysteme," *at - Automatisierungstechnik*, vol. 64, no. 10, pp. 806–815, Oct. 2016.

[17] T. Hulin, C. Preusche, and G. Hirzinger, "Stability boundary for haptic rendering: Influence of physical damping," in *Proc. IEEE/RSJ Int. Conf. Intell. Robots Syst.*, Oct. 2006, pp. 1570–1575.

[18] N. Hogan, "Controlling impedance at the man/machine interface," in *Proc. Int. Conf. Robot. Autom.*, May 1989, pp. 1626–1631.

[19] M. Dyck, A. Jazayeri, and M. Tavakoli, "Is the human operator in a teleoperation system passive?" in *Proc. World Haptics Conf.*, Apr. 2013, pp. 683–688.

[20] S. P. Buerger, H. I. Krebs, and N. Hogan, "Characterization and control of a screw-driven robot for neurorehabilitation," in *Proc. IEEE Int. Conf. Control Appl.*, Aug. 2001, pp. 388–394.

[21] P. Agarwal and A. D. Deshpande, "Impedance and force-field control of the index finger module of a hand exoskeleton for rehabilitation," in *Proc. IEEE Int. Conf. Rehabil. Robot.*, Aug. 2015, pp. 85–90.

[22] B. Ding, Q. Ai, Q. Liu, and W. Meng, "Path control of a rehabilitation robot using virtual tunnel and adaptive impedance controller," in *Proc. 7th Int. Symp. Comput. Intell. Des.*, Dec. 2014, vol. 1, pp. 158–161.

[23] T. Tsumugiwa, R. Yokogawa, and K. Hara, "Variable impedance control based on estimation of human arm stiffness for human-robot cooperative calligraphic task," in *Proc. IEEE Int. Conf. Robot. Autom.*, May 2002, vol. 1, pp. 644–650.

[24] K. Gu, "A further refinement of discretized Lyapunov functional method for the stability of time-delay systems," *Int. J. Control*, vol. 74, no. 10, pp. 967–976, Nov. 2001.

[25] K. Gu, V. Kharitonov, and J. Chen, *Stability of Time-Delay Systems*. Cambridge, MA, USA: Birkhäuser, 2003.

[26] J.-P. Corriou, *Process Control-Theory and Applications*. New York, NY, USA: Springer, 2004.

[27] A. Hurwitz, "Über die Bedingungen, unter welchen eine Gleichung nur Wurzeln mit negativen reellen Teilen besitzt," *Math. Ann.*, vol. 46, no. 2, pp. 273–284, 1895, English translation "On the conditions under which an equation has only roots with negative real parts by H. G. Bergmann," in *Selected Papers on Mathematical Trends in Control Theory*, R. Bellman and R. Kalaba, Eds. New York, NY, USA: Dover, 1964, pp. 70–82.

[28] A. Papachristodoulou, "Analysis of nonlinear time-delay systems using the sum of squares decomposition," in *Proc. Amer. Control Conf.*, Jun. 2004, vol. 5, pp. 4153–4158.

[29] P. Park, "A delay-dependent stability criterion for systems with uncertain time-invariant delays," *IEEE Trans. Autom. Control*, vol. 44, no. 4, pp. 876–877, Apr. 1999.

[30] Y. S. Lee, Y. S. Moon, and W. H. Kwon, "Delay-dependent guaranteed cost control for uncertain state-delayed systems," in *Proc. Amer. Control Conf.*, Jun. 2001, vol. 5, pp. 3376–3381.

[31] J.-J. E. Slotine and W. Li, *Applied Nonlinear Control*. Englewood Cliffs, NJ, USA: Prentice-Hall, 1991.

[32] B. Petreska and A. Billard, "Movement curvature planning through force field internal models," *Biol. Cybern.*, vol. 100, no. 5, pp. 331–350, May 2009.

[33] J. Chen and H. A. Latchman, "Frequency sweeping tests for stability independent of delay," *IEEE Trans. Autom. Control*, vol. 40, no. 9, pp. 1640–1645, Sep. 1995.

[34] V. Duchaine, B. Mayer-St-Onge, D. Gao, and C. Gosselin, "Stable and intuitive control of an intelligent assist device," *IEEE Trans. Haptics*, vol. 5, no. 2, pp. 148–159, Apr.–Jun. 2012.

[35] F. Müller, J. Janetzky, U. Behrnd, J. Jäkel, and U. Thomas, "User force-dependent variable impedance control in human-robot interaction," in *Proc. 14th IEEE Int. Conf. Autom. Sci. Eng.*, Aug. 2018, pp. 1328–1335.

Jens Jäkel received the diploma degree in electrical engineering from Leipzig Technical University, Leipzig, Germany, in 1994, and the Ph.D. degree in control engineering from Karlsruhe University, Karlsruhe, Germany, in 1999.

Since 2005, he has been working as a Professor for system theory and mechatronics with the Leipzig University of Applied Science. His research interests include model-based control design of mechatronic systems and machine learning.

Jozef Suchý received the Ing. and Ph.D. degrees in electrical engineering from the Slovak University of Technology in Bratislava, Bratislava, Slovakia, in 1973 and 1978, respectively.

Until 1996, he was with the Institute of Control Theory and Robotics, Slovak Academy of Science, Bratislava. Until April 2015, he was a Professor and the Head of the Department of Robotic Systems, Faculty of Electrical Engineering and Information Technology, University of Technology Chemnitz, Germany. Since April 2015, he has been working with the Department of Computer Science, Faculty of Natural Science, University of Matej Bel, Bansk Bystrica, Slovakia.

Florian Müller received the B.Eng. degree in electrical engineering and the master's degree in electrotechnical engineering from the Leipzig University of Applied Science, Leipzig, Germany, in 2011 and 2013, respectively, and the Ph.D. degree from the Chemnitz University of Technology, Chemnitz, Germany, in 2019.

He is currently working as a Postdoc with the Chair of Robotics and Human-Machine-Interaction Lab, the Chemnitz University of Technology. His research interests include the physical human–robot interaction, stability of nonlinear time-delay systems, force control, and biped robots.

Ulrike Thomas received the Diploma degree in computer science in 2000 and the Ph.D. degree in 2008 in robotics both from the Institute of Robotics and Process Control, Technical University of Braunschweig, Braunschweig, Germany.

From 2007 to 2015, she was with the Robotics and Mechatronics Institute, German Aerospace Center, Weßling, Germany. Since 2015, she has been a Professor and Lead of the Robotics and Human-Machine-Interaction Lab, Chemnitz University of Technology, Chemnitz, Germany. Her research interests are in the field of production technology and service robotics, which include human–machine interfaces for robots, control architectures, automated assembly planning, and machine learning as well as computer vision for robotics.